

Effect of Cholesterol, Fatty Acyl Chain Composition, and Bilayer Curvature on the Interaction of Cytochrome *b*₅ with Liposomes of Phosphatidylcholines[†]

Kenneth M. P. Taylor and Mark A. Roseman*

Department of Biochemistry, Uniformed Services University of the Health Sciences, Bethesda, Maryland 20814-4799

Received July 21, 1994; Revised Manuscript Received November 18, 1994[®]

ABSTRACT: To determine the effect of cholesterol and lipid packing on the solubility of membrane proteins in bilayers, cytochrome *b*₅ incorporation into phosphatidylcholine (PC) liposomes was determined as a function of bilayer curvature (SUVs versus LUVs), fatty acyl chain composition, and cholesterol content. The equilibrium affinity constant for the formation of a 1:1 *b*₅/PC complex, *K*_p, and the number of PC's per "site" at saturation, *n*, were determined from binding isotherms, which were obtained by measuring the increase in intrinsic tryptophan fluorescence. With LUVs, *n* was also determined directly by gel filtration. The following results were obtained: (1) Both *K*_p and the saturating level of *b*₅ binding, *s* (*n*⁻¹), are significantly greater for SUVs than for LUVs. In LUVs, a binding site must consist of several surrounding lipid layers. (2) Cholesterol reduces *K*_p and *s* by factors that range from 1 to >100. Binding inhibition is highly sensitive to the liposome size and to the fatty acyl composition of the PC; the latter correlates with the condensing effects on PC: C1_{sat}C2_{mono} > C1_{sat}C2_{di} ≈ natural mixtures > C1_{unsat}C2_{unsat}. (3) With POPC LUVs, the binding inhibition was 3.6-, 1.4-, and 17-fold within the ranges of 0–20, 20–33, and 33–50 mole percent cholesterol, respectively. (4) The equilibrium binding constant to SUVs is greater for liposomes that are prepared from natural PC mixtures than for vesicles of a single synthetic phospholipid. The reductions in *b*₅ binding correlate with reductions in bilayer free volume, which were calculated from monolayer studies of the lipid mixtures. The sensitivity of liposome saturability to bilayer curvature, fatty acyl chain composition, and cholesterol content may account for the disparate results among previous studies of cholesterol–protein interactions. A more significant implication is that in biological membranes with high levels of cholesterol, subtle variations in the fatty acyl chain composition could substantially affect the solubility and physical states of integral membrane proteins.

The importance of lipid composition on the solubility of integral membrane proteins in the lipid phase remains a fundamental problem in membrane biophysical chemistry. Since cholesterol is a major lipid component with the most pronounced effects on bilayer physical properties at physiological temperatures, studies involving the effects of cholesterol on protein–lipid and protein–protein interactions may be the most relevant in answering this question.

The most direct approach has been to observe the effect of cholesterol on protein aggregation, which can be determined either from the clustering of intramembranous particles or from a decrease in protein rotational mobility. By fusing inner mitochondrial vesicles with cholesterol-containing liposomes, Hochli *et al.* (1980) were able to increase the amount of cholesterol in the mitoplast membranes. Above 30% cholesterol, aggregation of intramembrane particles became evident. A similar study was performed by Cherry *et al.* (1980) with bacteriorhodopsin reconstituted into liquid-crystalline DMPC liposomes. In this case, aggregation of intramembrane particles, concomitant with a decrease of protein rotational mobility, was induced by membrane cholesterol compositions of only 10 mole percent. Cholesterol-induced aggregation of band 3 in erythrocyte membranes

was also inferred from a decrease in protein rotational mobility as the bilayer cholesterol content was increased from 32.4 to 59.3 mole percent by incubation with cholesterol-rich liposomes (Muhleback & Cherry, 1982). Collectively, these studies indicate that cholesterol decreases the solubility of proteins in the lipid phase, although the cholesterol composition at which this occurs may vary significantly among different systems.

A different approach was taken by Yeagle (1984). In reconstitution studies of glycophorin with egg phosphatidylcholine (PC)¹ and cholesterol, all recombinant vesicles had output cholesterol/PC ratios essentially identical to the input ratios within the range of 0–60 mole percent cholesterol. This suggests, in contrast to the aggregation studies described above, that PC and cholesterol have comparable affinities for the protein.

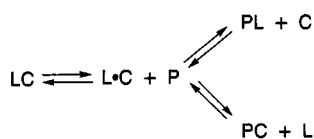
¹ Abbreviations: DOPC, 1,2-dioleoyl-*sn*-glycero-3-phosphocholine; DLPC, 1,2-dilinoleoyl-*sn*-glycero-3-phosphocholine; POPC, 1-palmitoyl-2-oleoyl-*sn*-glycero-3-phosphocholine; SOPC, 1-stearoyl-2-oleoyl-*sn*-glycero-3-phosphocholine; PLPC, 1-palmitoyl-2-linoleoyl-*sn*-glycero-3-phosphocholine; SLPC, 1-stearoyl-2-linoleoyl-*sn*-glycero-3-phosphocholine; egg PC, egg L-α-phosphatidylcholine; liver PC, bovine liver L-α-phosphatidylcholine; PE, phosphatidylethanolamine; SPH, bovine brain sphingomyelin; [¹⁴C]POPC, L-α-1-palmitoyl-2-oleoyl[¹⁴C]oleoyl-1-¹⁴C]phosphatidylcholine; [³H]triolein, [9,10-³H(N)]triolein; cyt *b*₅, cytochrome *b*₅; Tris, tris(hydroxymethyl)aminomethane; Bicine, *N,N*-bis(2-hydroxyethyl)glycine; EDTA, ethylenediaminetetraacetic acid; TNBS, 2,4,6-trinitrobenzenesulfonic acid; LUV, large unilamellar vesicle; SUV, small unilamellar vesicle; ϕ , cholesterol inhibitory parameter; PC, phosphatidylcholine; PL, phospholipid.

[†] Supported by USUHS Protocols C071AH and T071A0.

* To whom correspondence should be addressed at the Department of Biochemistry, Uniformed Services University of the Health Sciences, 4301 Jones Bridge Rd., Bethesda, MD 20814-4799. Telephone: (301) 295-3570.

[®] Abstract published in *Advance ACS Abstracts*, February 1, 1995.

Scheme 1



The relative affinities of lipids in a mixture for the boundary layer surrounding a protein also have been investigated. Using spin-labeled PC and spin-labeled cholesterol, Silvius *et al.* (1984) observed that PC has no greater affinity for the annulus of the sarcoplasmic Ca^{2+} -ATPase than it does for the bulk lipid phase; cholesterol, in the presence of excess PC, prefers the bulk phase, but only by a modest factor of 1.54. As these authors suggest, this result could be interpreted either as (1) cholesterol binds to 65% of the annular sites with the same affinity as a phospholipid or (2) cholesterol binds to all of the annular sites with about 0.65 of the affinity as a phospholipid.

A similar study of Ca^{2+} -ATPase utilized brominated derivatives of both PC and cholesterol, which are collisional quenchers of the protein's intrinsic tryptophan fluorescence (Simmonds *et al.*, 1982). In this case, the two lipids displayed noncompetitive interaction with the protein, suggesting that specific, mutually exclusive annular binding sites exist for cholesterol and PC. Although these results do not seem compatible with those using spin-labeled lipids, the apparent discrepancies may be rationalized by taking into account the large differences in cholesterol:PC ratios that were used, as will be discussed later.

The results of annular lipid competition experiments, though useful and informative, cannot necessarily be used to determine the full effect of cholesterol on the solubility of a protein in a membrane. Consider the pairwise interactions of the three components of the phospholipid/cholesterol/protein ternary mixture, as shown in Scheme 1 where P, C, and L are protein, cholesterol, and phospholipid. L·C is a hypothetical ideal mixture of L and C in a lipid bilayer whereas LC is a more closely packed, condensed phospholipid/cholesterol phase, as is known to exist in certain phospholipid/cholesterol mixtures. PC and PL respectively represent protein in contact with annular cholesterol and phospholipid. Whatever the relative affinities of cholesterol and phospholipid are for the annulus, if the protein is insoluble in the condensed phase, addition of cholesterol would decrease the observed saturation level of the protein in the lipid mixture by reducing the amount of phospholipid that could interact with the protein.

Evidently, a definitive conclusion does not emerge from the studies which have been performed. To obtain quantitative information about the effect of cholesterol and bilayer physical properties on the chemical potential of intrinsic proteins in a membrane, the ideal system to study would be one in which the protein readily partitions between the aqueous phase and the membrane. Although binding isotherms have been experimentally obtained with amphipathic helical oligopeptides, which generally bind to the surfaces or interfaces of lipid bilayers, most proteins that actually penetrate into the bilayer core do not have sufficient aqueous solubility for such an approach to be taken. However, a notable exception is cytochrome b_5 .

Cytochrome b_5 is an amphipathic protein with two independent domains: a 12 000 Da, negatively charged

aqueous-soluble catalytic domain at the amino terminus and a hydrophobic 4 000 Da membrane-anchoring domain in the carboxy-terminal region [reviewed by Strittmatter and Dailey (1982)]. The purified protein is water-soluble in the absence of detergent, existing as an equilibrium mixture of octomers and monomers (Calabro *et al.*, 1976). When added to most preformed membranes and liposomes, the monomers spontaneously bind to the outer monolayer (Strittmatter *et al.*, 1972; Enomoto & Sato, 1973; Dufourq *et al.*, 1974; Sullivan & Holloway, 1974; Holloway & Katz, 1975; Rogers & Strittmatter, 1975; Remacle, 1978). This simple reconstitution method usually produces a form of the protein designated "loose," which is transferrable between liposome populations (Roseman *et al.*, 1977; Enoch *et al.*, 1979) via an aqueous diffusion mechanism (Leto *et al.*, 1988). In contrast, the physiological binding form of cyt b_5 , referred to as "tight," is nontransferrable among membranes (Enoch & Strittmatter, 1979). Tight insertion can be obtained quantitatively in liposomes either by reconstituting with detergents (Enoch *et al.*, 1979; Poensgen & Ullrich, 1980; Christiansen & Carlson, 1986) or by incubating liposomes with loosely bound protein at high temperatures (Ladokhin *et al.*, 1993). Studies in this laboratory have shown that the conditions for formation of the two binding forms are not so restrictive; spontaneous incorporation of cyt b_5 always results in an initial, small but significant level of tight binding, which subsequently increases over a period of days (Greenhut *et al.*, 1986, 1993).

In the loose configuration, the nonpolar domain forms a hairpin structure. However, the depth to which it penetrates into the bilayer is not firmly established, having been reported as 20 Å (Takagaki *et al.*, 1983; Kleinfeld & Lukacovic, 1985) or 7 Å (Tennyson & Holloway, 1986). Figure 1 depicts a model of the loosely bound membrane-anchoring domain that is inserted to a depth of 20 Å. Similarly, there is still controversy about the overall topology of the tail when it is inserted in the tight configuration, i.e., whether it spans the membrane or forms a helical hairpin similar to that of the loose configuration.

In the present investigation, we have measured the binding of cyt b_5 to PC liposomes of different curvature, fatty acyl composition, and cholesterol content. All three factors, independently and cooperatively, substantially affect the partitioning of this protein into preformed bilayers. The results are consistent with a simple model in which the extent of binding depends upon bilayer free volume.

Preliminary reports of our results have been presented (Taylor & Roseman, 1990, 1993).

EXPERIMENTAL PROCEDURES

Materials. 1,2-Dioleoyl-*sn*-glycero-3-phosphocholine (DOPC), 1,2-dilinoyleoyl-*sn*-glycero-3-phosphocholine (DLPC), 1-palmitoyl-2-oleoyl-*sn*-glycero-3-phosphocholine (POPC), 1-stearoyl-2-oleoyl-*sn*-glycero-3-phosphocholine (SOPC), 1-palmitoyl-2-linoleoyl-*sn*-glycero-3-phosphocholine (PLPC), 1-stearoyl-2-linoleoyl-*sn*-glycero-3-phosphocholine (SLPC), egg L- α -phosphatidylcholine (egg PC), bovine liver L- α -phosphatidylcholine (liver PC), transphosphatidylated phosphatidylethanolamine, prepared from egg PC (PE), and bovine brain sphingomyelin (SPH) (all >99% purity) were purchased from Avanti Polar Lipids (Alabaster, AL). Highly purified (>99%) cholesterol was from Calbiochem Corp. (La

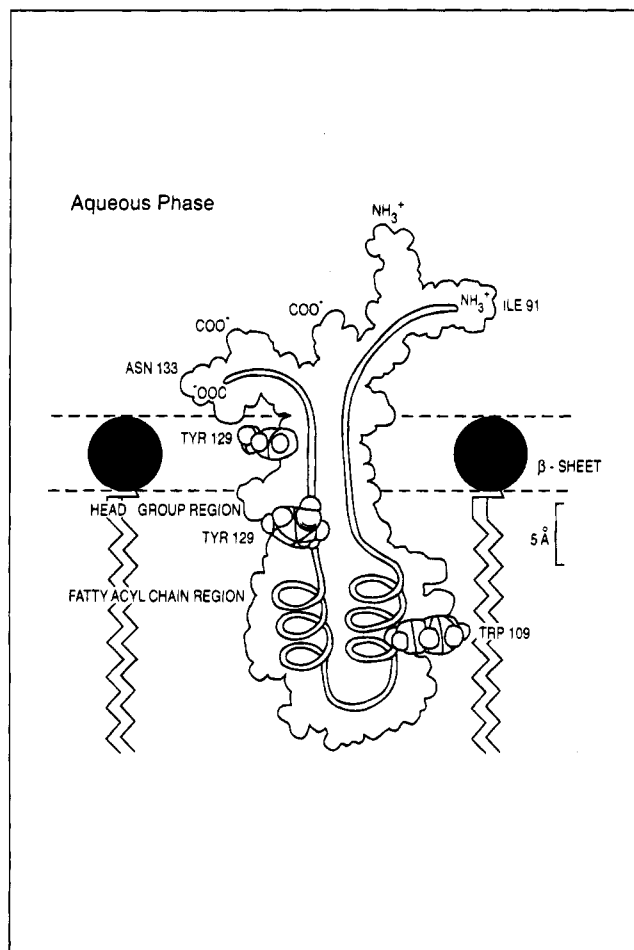


FIGURE 1: Structure of the cytochrome *b*₅ membrane anchoring domain. The model is adapted from Strittmatter and Dailey (1982).

Jolla, CA). Lipids were used without further purification. [¹⁴C]POPC (specific activity, 58.0 μ Ci/ μ mol) and [³H]triolein (specific activity, 2.68×10^4 μ Ci/ μ mol) were from New England Nuclear.

Cytochrome *b*₅, from bovine liver, was purified to homogeneity as described by Greenhut and Roseman (1985).

Preparation of Large Unilamellar Vesicles (LUVs). Lyophilized phospholipids and cholesterol (100–200 μ mol of total lipid) along with 1.0 μ Ci of [¹⁴C]POPC or [³H]triolein were codissolved in 5–10 mL of chloroform. Chloroform was removed by rotary evaporation followed by lyophilization from benzene under high vacuum for 12 h. Liposome dispersions were obtained by reverse-phase evaporation (Düzgünes *et al.*, 1983), using 20 mM Tris–acetate, 100 mM NaCl, and 0.1 mM EDTA, pH 8.1, as the aqueous phase. The initially formed liposomes were extruded through consecutive polycarbonate membranes (Nuclepore) with pore sizes of 0.4, 0.2, 0.1, and 0.08 μ m. For vesicles consisting of ≥ 30 mole percent cholesterol, a model HPVE-10 high-pressure extrusion apparatus (Sciema Technical Ltd., Vancouver, Canada) was used to facilitate liposome extrusion. Contaminating small and intermediate size vesicles were removed from the preparation by gel-filtration through a Sepharose 2B-CL column (1.6 \times 55 cm); only the peak void-volume fractions were collected (Greenhut *et al.*, 1986). Lipid phosphorous was determined according to the Bartlett (1959) method.

The fraction of total lipid on the exterior liposome surfaces was determined with separate preparations: Liposomes of

which PE comprised 10 mole percent of the total phospholipid were prepared as above in 40 mM Bicine, 10 mM NaCl, and 0.1 mM EDTA, pH 8.5. The relative out:in lipid mass ratios were obtained from the PE reactivity with 2,4,6-trinitrobenzenesulfonate (Fluka Chemika-Biochimika) as previously described elsewhere (Greenhut & Roseman, 1985). The liposome preparations \pm 50 mole percent cholesterol typically had out:in ratios of 0.7, indicating that approximately 80% of the total lipid forms exposed bilayers and 20% is sequestered within oligolamellar structures.

Preparation of Small Unilamellar Vesicles (SUVs). Approximately 100–200 μ mol of total lipid (phospholipid \pm cholesterol) was dissolved in chloroform, dried to a film by rotary evaporation, and then lyophilized from 5 mL of benzene under high vacuum for a minimum of 12 h. The dried lipid was subsequently hydrated with 11 mL of Tris–acetate buffer, pH 8.1, transferred to a 15 mL Corex tube, and sonicated (W-375 Heat Systems–Ultrasonics sonicator, 0.5-in. probe, 50% pulsed duty cycle) to constant clarity under argon. Constant temperature was maintained above the phospholipid gel–liquid-crystalline phase transition during sonication with a water bath. Homogeneous populations of limit-size vesicles were obtained by differential sedimentation (Ti50 fixed-angle rotor, 45 000 rpm, 1 h) of contaminating larger vesicles (Barenholz *et al.*, 1977). TNBS-labeling of selected preparations with 9:1 PC/PE showed these liposomes to be unilamellar with 62% of the total lipid localized in the exterior monolayer.

Cytochrome *b*₅ Saturation of Large Unilamellar Vesicles. Detergent-free cyt *b*₅ and preformed LUVs were incubated at 30 or 37 $^{\circ}$ C in Tris–acetate buffer for prolonged periods of 24 h under argon. Initial incubation ratios varied from 1:40 to 1:417 cyt *b*₅ per phospholipid. The extent of cyt *b*₅ binding was determined by separating the proteoliposomes from unbound protein with Sepharose 2B-CL columns (0.9 \times 28.5 cm if 2 μ mol of phospholipid was used, or 1.6 \times 55 cm if 5–20 μ mol of phospholipid was used). Cyt *b*₅ was assayed according to the method of Greenhut *et al.* (1986): to fraction samples in 900 μ L of Tris–acetate buffer was added 100 μ L of 10% (w/w) deoxycholate (to eliminate light scattering by the liposomes), and the absorption spectra were obtained over the range 350–500 nm with an SLM-Aminco DW-2C spectrophotometer. The concentration of cyt *b*₅ was calculated using a molar extinction coefficient of 1.17×10^5 M⁻¹ cm⁻¹ at 413 nm (Spatz & Strittmatter, 1971). Elution profiles of ¹⁴C- or ³H-labeled liposomes were determined from the isotope disintegrations (60 s counting time) of fraction samples using Beckman HP liquid scintillation cocktail. The extent of binding was determined from the percent of cyt *b*₅ from the initial incubation mix that eluted with the liposomes.

Cytochrome *b*₅ Saturation of Small Unilamellar Vesicles. The saturation limits of SUVs were determined from the enhancement in cyt *b*₅ intrinsic tryptophan fluorescence (Dufourcq *et al.*, 1975; Leto & Holloway, 1979). Separate samples of cyt *b*₅ (1.56 μ M) with variable lipid concentration (0–0.624 mM phospholipid) were incubated for 2 h at 25 or 37 $^{\circ}$ C, in Tris–acetate buffer, pH 8.1. Fluorescence spectra were obtained in a magnetically stirred cuvette, thermostated at either 25 $^{\circ}$ C or 37 $^{\circ}$ C, with an SLM-Aminco SPF-500 spectrofluorometer operating in the ratio mode. Excitation and emission wavelengths were 280 and 338 nm; bandwidths were 2.5 and 5 nm, respectively. When ap-

appropriate, cyt b_5 fluorescence spectra were adjusted for light scattering by subtracting the spectral scattering intensities of vesicles alone at the corresponding concentrations. The maximum total lipid concentration (1.25 mM) was not sufficient to significantly attenuate the incident light beam [Leto and Holloway (1979) and references cited therein]. The fraction of liposome-bound cyt b_5 was quantitated according to the formula:

$$X_{BD} = 1 - (F_{BD} - F_{OBS}) / (F_{BD} - F_{UBD}) \quad (1)$$

where X_{BD} is the fraction of bound protein, F_{BD} is the end point fluorescence of cyt b_5 obtained in the presence of excess lipid, F_{UBD} is cyt b_5 fluorescence in the absence of liposomes, and F_{OBS} is the fluorescence of cyt b_5 during the titration course of increasing lipid concentration (Leto & Holloway, 1979).

Analysis of Cytochrome b_5 Binding Isotherms. Cyt b_5 binding data were replotted according to Scatchard (1949). The plots were analyzed according to an iterative curve-fitting routine of a nonlinear model which considers the membrane surface as a two-dimensional lattice for large-ligand adsorption. This general equation has been previously formulated as:

$$r/C_A = K_{eff}(1 - nr) \left[1 - \frac{\lambda nr}{1 + nr(\lambda - 1)} \cdot \frac{2}{q + 1} \right]^\gamma \quad (2)$$

where

$$q = \{1 + 4\lambda nr(\eta - 1)(1 - nr) / [1 - nr(1 - \lambda)]^2\}^{1/2} \quad (3)$$

where r represents the solution concentration mole ratio of bound ligand per total phospholipid, C_A is the concentration of free ligand, K_{eff} is an effective or apparent affinity constant for a binding site, n is the minimum number of lipid molecules that constitute an adsorption site, and λ , γ , and η are statistical parameters that respectively account for lattice geometry, ligand shape, and the type and extent of cooperativity (Stankowski, 1984). In a plot of r/C_A vs r , eq 2 generates a negatively curved function with respective ordinate and abscissa intercepts of K_{eff} and $1/n$.

An applicable equation for cyt b_5 interaction with liposomes was obtained by initially determining the limiting binding parameters (i.e., the minimum stoichiometric number of phospholipids per protein). The binding of cyt b_5 monomers to liposome surfaces was modeled upon the following assumptions: (1) The cyt b_5 catalytic domain, a prolate ellipsoid with dimensions $25 \text{ \AA} \times 25 \text{ \AA} \times 32 \text{ \AA}$ (Mathews *et al.*, 1972), covers approximately $491\text{--}628 \text{ \AA}^2$ on the bilayer surface, depending upon its rotational orientation. For simplicity, the greater surface area was selected for modeling of the binding lattice so that the precise domain alignment could be disregarded. (2) The average phospholipid molecular area is approximately $65\text{--}70 \text{ \AA}^2$. Since a cyt b_5 adsorption site would apparently require 9–10 phospholipids, the liposome surface was modeled as a stretched hexagonal lattice with a single contour shell ($p = 1$) of eight phospholipids circumscribing a linear sequence of two additional phospholipid molecules ($k = 2$), and with overall dimensions of $a = 4$ phospholipids in length ($a = k + 2p$) and $b = 3$ phospholipids ($b = 2p + 1$) in breadth. The statistical parameters λ , α (the excluded surface area that becomes unavailable for additional ligand adsorption), and γ

for this particular lattice were determined from the previously derived formulae for stretched hexagons (Stankowski, 1984):

$$n\lambda = [2(a + p) + 1]/3 \quad (4)$$

$$n\alpha = [2a^2 - p^2 + 10ap - 7p - a - 1]/3 \quad (5)$$

$$\gamma = \alpha/\lambda \quad (6)$$

Inserting $a = 4$ and $p = 1$ into the above equations and then substituting for λ , α , and γ in eqs 2 and 3 with simplification give an expression that mathematically describes cyt b_5 binding to liposomes:

$$r/C_A = K_{eff}(1 - nr) \left[1 - \frac{3.7r}{1 + 3.7r - nr} \cdot \frac{2}{q + 1} \right]^{5.3} \quad (7)$$

with

$$q = [1 + 14.8r(\eta - 1)(1 - nr) / (1 + 3.7r - nr)^2]^{1/2} \quad (8)$$

Fitting of eq 7 to experimental data was performed by an iterative process in which K_{eff} , n , and η were varied as free parameters. The set of parameters which gave the best curve-fit to the data were assumed to be the solutions of the binding function. To obtain reasonable fits for these plots, cooperativity parameters that are substantially less than unity needed to be assumed: solutions for η were typically 0.64 ± 0.03 . The results obtained for η indicate that cyt b_5 insertion into SUVs may be an anticooperative process; the binding of each cyt b_5 to the liposome surface decreases the affinity of remaining unbound molecules. Anticooperative binding is predicted for cytochrome b_5 , resulting from electrostatic repulsion between the highly negatively charged catalytic domains.

A complication in determining reliable measures of K_{eff} arises from the possibility [based upon past studies with LUVs (Greenhut *et al.*, 1986, 1993)] that a minor but significant fraction of the cyt b_5 binds to the SUVs in the tight configuration. If so, this population of tightly bound protein would be manifest in a Scatchard plot as an increased curvature at low r and an enhanced y-axis intercept. This possibility was explored by systematically deleting several points from low r , and comparing the curve fit to the remaining points with that of the original. The differences were not significant (data not shown).

Having two binding forms of a ligand should not affect the determined value of n in a Scatchard plot, so long as each form requires the same number of phospholipids per site. As will be shown under Results, the plots are in fact valid measures of n .

RESULTS

Cyt b_5 Binding to SUVs. Representative binding isotherms of cyt b_5 with SUVs are shown in Figure 2. As cyt b_5 is incubated with increasing amounts of phospholipid there is a stoichiometric uptake of protein until complete binding occurs. With egg PC SUVs, the binding isotherm exhibits a defined breakpoint at approximately 20 phospholipids per cyt b_5 (panel A, open circles). This result, which is typical of the phospholipids with a heterogeneous mixture of acyl chains, gives the appearance of irreversible binding, or at least of affinity constants that are too large to determine. However, when the SUVs contain 50 mole percent cholest-

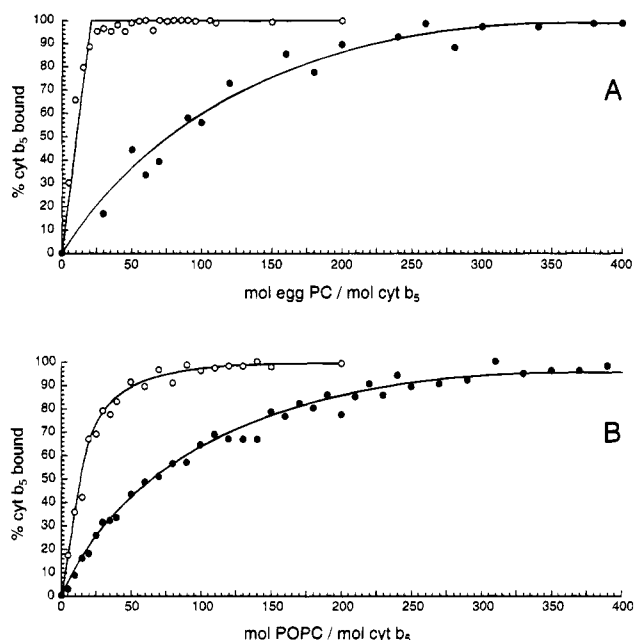


FIGURE 2: Cytochrome *b*₅ binding to SUVs. (A) Egg PC SUVs. Separate samples containing cyt *b*₅ (3.12 nmol) and liposomes (0–1.248 μ mol phospholipid) were incubated in a total volume of 2 mL of Tris–acetate buffer for 2 h at 25 °C. The extent of binding in each sample was then quantitated from the cyt *b*₅ fluorescence spectra using eq 1. The excitation wavelength was 280 nm, and the emission was recorded from 300 to 400 nm. Bandwidths were 2.5 and 5 nm. Fluorescence spectra were corrected for light scattering as described under Experimental Procedures. (○) SUVs with 0% cholesterol; (●) SUVs containing 50% cholesterol. (B) POPC SUVs. The protocol was the same as in (A).

terol, a definite curvature is evident, indicating a measurable equilibrium between octomer and bound protein (panel A, filled circles). With pure synthetic phospholipids such as POPC (which is also the major component of egg PC), a defined curvature in the cyt *b*₅ binding isotherm is also evident (panel B, open circles). As with the natural mixtures, the curvature becomes more pronounced when the vesicles contain cholesterol (panel B, filled circles).

Where a measurable equilibrium was evident, a nonlinear Scatchard analysis was used to determine the affinity

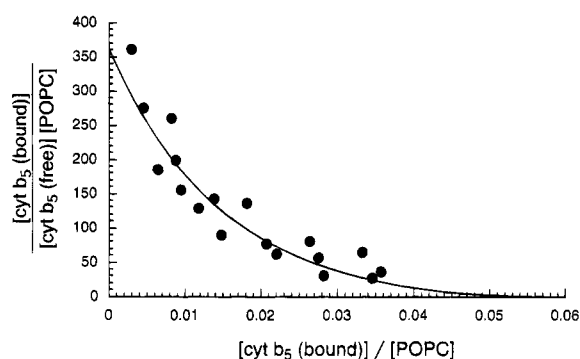


FIGURE 3: Scatchard plot of cytochrome *b*₅ binding to POPC SUVs; 0% cholesterol. The data for cyt *b*₅ binding to POPC SUVs (Figure 2B) were replotted as $r/[\text{unbound cyt } b_5] \text{ (mM}^{-1})$ vs r , where r is the molar solution concentration ratio of bound cyt *b*₅ per phospholipid ($[\text{bound cyt } b_5]/[\text{PL}]$). The curve is a fit of eq 7 that was obtained with solutions of $K_{\text{eff}} = 362 \text{ mM}^{-1}$ (y-axis intercept), $n = 16.7$ (reciprocal of x-axis intercept), and $\eta = 0.63$.

constants and the saturation levels of binding, as described under Experimental Procedures. A representative plot is shown for POPC SUVs (Figure 3). The ordinate intercept corresponds to the affinity constant and the abscissa intercept indicates the saturation ratio of cyt *b*₅ per phospholipid.

Cyt *b*₅ interaction with SUVs that are prepared from various phospholipids, with and without cholesterol, is summarized in Table 1. The parameter ϕ is the ratio of the relative cyt *b*₅ saturation limits of liposomes without cholesterol to liposomes with cholesterol, and is therefore a measure of the inhibitory effect of cholesterol. The maximum levels of binding are expressed as moles of cyt *b*₅ per 1000 mol of phospholipid, rather than as moles of cyt *b*₅ per mole of total lipid. Consequently, a value of $\phi < 1.0$ is expected if cholesterol participates in cyt *b*₅ binding, $\phi = 1.0$ if cholesterol does not participate in the binding, and $\phi > 1.0$ if cholesterol inhibits phospholipids from interacting with the protein. Since the surface areas of PC and cholesterol are approximately 70 Å² and 40 Å², respectively, PC would occupy approximately 64% of the area in a hypothetical ideal equimolar mixture of PC and cholesterol. Therefore, if protein interaction with the bilayer only

Table 1: Cytochrome *b*₅ Interaction with Phosphatidylcholine Small Unilamellar Vesicles^a

phospholipid	cholesterol (mol %)	$K_{\text{eff}}^b (\times 10^4) (\text{M}^{-1})$	n^c	$K_p^d (\times 10^3) (\text{M}^{-1})$	s^e (cyt <i>b</i> ₅ /1000 PL)	ϕ^f
DOPC	0	90 ± 9	16.7 ± 0.9	54 ± 5	60 ± 3	1.1 ± 0.06
	50	60 ± 5	17.9 ± 0.6	34 ± 3	56 ± 2	
DLPC	0	11.4 ± 0.9	17.5 ± 0.7	6.5 ± 0.5	57 ± 2	1.0 ± 0.05
	50	13 ± 1	17.5 ± 0.8	7.2 ± 0.6	57 ± 2	
POPC	0	36 ± 3	17 ± 1	22 ± 2	60 ± 4	4.6 ± 0.4
	50	8.1 ± 0.9	77 ± 3	1.1 ± 0.1	13 ± 0.5	
SOPC	0	23 ± 2	17 ± 1	14 ± 1	60 ± 3	3.2 ± 0.2
	50	16 ± 1	53 ± 1	3.0 ± 0.2	19 ± 0.4	
PLPC	0	11 ± 1	16.7 ± 0.6	6.4 ± 0.6	60 ± 2	1.9 ± 0.2
	50	9.8 ± 0.9	32 ± 1	3.0 ± 0.3	31 ± 1	
SLPC	0	9.4 ± 0.7	17.9 ± 0.9	49 ± 1	53 ± 3	1.6 ± 0.1
	50	11 ± 1	30 ± 1	3.6 ± 0.3	33 ± 1	
egg PC	0	>1000	21.3 ± 0.8 ^g	>500	47 ± 2	4.9 ± 0.3
	50	30 ± 4	105 ± 3	2.8 ± 0.4	9.5 ± 0.3	
liver PC	0	>1000	20.0 ± 0.8 ^g	>500	50 ± 2	5.4 ± 0.3
	50	26 ± 3	109 ± 3	2.4 ± 0.3	9.0 ± 0.3	
PC/SPH (1:1)	0	>1000	20.0 ± 0.8 ^g	>500	50 ± 2	5.3 ± 0.4
	50	25 ± 3	106 ± 6	2.3 ± 0.3	9.4 ± 0.5	

^a Binding parameters were determined from the Scatchard analysis (see text for details). ^b Effective affinity constant for a binding "site" on a liposome. ^c Phospholipids per site. ^d Affinity constant for a phospholipid (K_{eff}/n). ^e Cyt *b*₅ saturation level of a liposome (n^{-1}). ^f Cholesterol inhibitory parameter, (cyt *b*₅ saturation in liposomes without cholesterol)/(cyt *b*₅ saturation in liposomes with cholesterol). ^g Determined directly from binding isotherms at the intersection of lines drawn through the plateau region and the linear binding region of the curve.

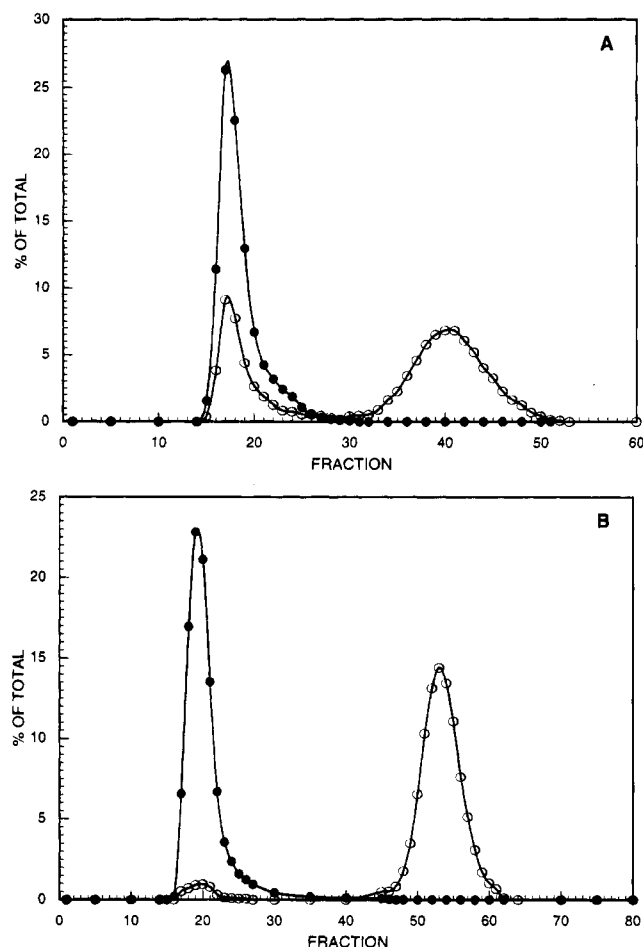


FIGURE 4: Saturation level of cytochrome b_5 binding to POPC LUVs. (A) 0% cholesterol. Cyt b_5 ($0.04 \mu\text{mol}$) and POPC liposomes ($2 \mu\text{mol}$ of POPC doped with $6.7 \times 10^4 \text{ dpm}$ of $[^{14}\text{C}]\text{POPC}/\mu\text{mol}$ of POPC) were incubated in a total volume of $422 \mu\text{L}$ of Tris-acetate buffer for 24 h at 30°C under argon. $390 \mu\text{L}$ of the incubation mixture was then applied to a Sepharose 2B-CL column ($0.9 \times 28.5 \text{ cm}$) equilibrated in Tris-acetate buffer, pH 8.1, and thermostated at 25°C . Fractions of $320 \mu\text{L}$ were collected and assayed for POPC (\bullet) and cyt b_5 (\circ). (B) 50% cholesterol. Cyt b_5 ($0.024 \mu\text{mol}$) was incubated with liposomes containing $10 \mu\text{mol}$ each of POPC and cholesterol (doped with $9.8 \times 10^4 \text{ dpm}$ of $[^{14}\text{C}]\text{POPC}/\mu\text{mol}$ of POPC) in a total volume of 1.76 mL . 1.60 mL of the incubation mixture was then applied to a Sepharose 2B-CL column ($1.6 \times 55 \text{ cm}$). Fractions of 1.60 mL were collected and assayed for cyt b_5 and POPC.

depended upon actual lipid area, the value of ϕ would be 0.64. The results show that in all cases $\phi \geq 1$, indicating that cholesterol does not participate in, or that it inhibits, cyt b_5 binding to SUVs.

The extent to which cholesterol influences cyt b_5 binding depends upon the phospholipid composition of the liposome: ϕ varies from 1.0 for single-chain diunsaturated phospholipids to approximately 5 for natural mixtures and mixed-chain phospholipids. The order essentially reflects the extent to which cholesterol condenses monolayers of the phospholipids, as will be discussed in more detail later.

The cyt b_5 affinity per phospholipid is generally more sensitive than the liposome saturation level to variations in fatty acyl chain composition or cholesterol content. For example, K_p of cyt b_5 for egg PC is greater than for POPC, the major component of the mixture, by at least a factor of 20; similarly, cholesterol reduces the affinity of the protein for egg PC by more than 20-fold.

Table 2: Saturation Levels of Cytochrome b_5 Binding in Phosphatidylcholine Large Unilamellar Vesicles^a

phospholipid	cytochrome <i>b</i> ₅ /1000 phospholipids				ϕ^d
	0% cholesterol		50% cholesterol		
	observed ^b	corrected ^c	observed	corrected	
DOPC	10.1	11.5	7.9	9.4	1.2
DLPC	17.2	17.2	16.3	16.7	1.0
POPC	6.8	9.0	0.1	0.1	90.0
SOPC	6.9	10.3	0.1	0.2	51.5
PLPC	16.6	21.9	1.4	1.8	12.2
SLPC	15.1	20.0	1.5	2.3	8.7
egg PC	13.9	19.4	1.2	1.6	12.1
liver PC	15.1	17.9	1.1	1.2	14.9
PC/SPH (1:1)	16.2	17.6	1.4	1.5	11.7

^a Cyt b_5 and ^{14}C -labeled liposomes were incubated for 24 h at 30 – 37°C under argon. Initial binding ratios from which $>25\%$ of the cyt b_5 remained unbound were assumed to contain saturating levels of protein. ^b The extent of binding was determined from the percentage of cyt b_5 eluting with liposomes in the void volume from a Sepharose 2B-CL column (see Experimental Procedures). ^c Cyt b_5 /phospholipid at saturation corrected for liposome lamellarity (determined by TNBS labeling). ^d Cholesterol inhibitory parameter, $\phi = (\text{cyt } b_5 \text{ saturation in liposomes without cholesterol})/(\text{cyt } b_5 \text{ saturation in liposomes with } 50\% \text{ cholesterol})$. ϕ is calculated from the corrected values. Replica experiments with selected liposome preparations showed these results to be reproducible to $\pm 4\%$.

Cyt b_5 Binding to LUVs. Figure 4 shows representative gel filtration elution profiles of mixtures containing LUVs (POPC in panel A and equimolar POPC/cholesterol in panel B) and excess cyt b_5 . The cyt b_5 -liposome complexes elute in the void volume, completely resolved from unbound protein. With this particular phospholipid, cholesterol markedly reduces the liposome saturation limit.

Table 2 summarizes the cyt b_5 saturation levels of LUVs that are prepared from various synthetic and natural phosphatidylcholines, ± 50 mole percent cholesterol. The cyt b_5 saturation limits of LUVs are severalfold less than those with SUVs. Qualitatively, the effect of cholesterol is the same as that observed with SUVs: $\phi \geq 1.0$ with all phospholipids, indicating that cholesterol either does not participate in or inhibits cyt b_5 partitioning into preformed bilayers. But with LUVs, the ϕ values exhibit a substantially broader range (1.0–70) and a more definitive trend with respect to the extent and position of fatty acyl chain unsaturation: $\text{C1}_{\text{sat}}\text{C2}_{\text{mono}} > \text{C1}_{\text{sat}}\text{C2}_{\text{di}} \approx \text{mixtures} > \text{C1}_{\text{unsat}}\text{C2}_{\text{unsat}}$.

A comparison of the results obtained with SUVs and LUVs shows the remarkable effect that bilayer curvature has on the overall binding of cyt b_5 to a liposome (Figure 5).

To further characterize the cholesterol inhibitory effect, cyt b_5 partitioning into POPC LUVs (the liposome system with the most pronounced cholesterol-mediated reduction in saturation level) was also investigated as a function of the cholesterol mole fraction. Cholesterol decreases the saturation level of cyt b_5 binding by factors of 3.6, 1.4, and 17, within the composition ranges of 0–20, 20–33, and 33–50 mole percent, respectively (Figure 6). The affinity constant per site is remarkably constant (Table 3); the reduction in affinity per phospholipid is due almost entirely to the increased number of phospholipids per site.

Effect of Cyt b_5 Tight Insertion on Liposome Saturation Limits. Although most of the cyt b_5 binds to LUVs in the loose configuration, recent studies in this laboratory have shown that a significant fraction is tightly inserted, and that the rate of tight insertion depends upon the lipid composition

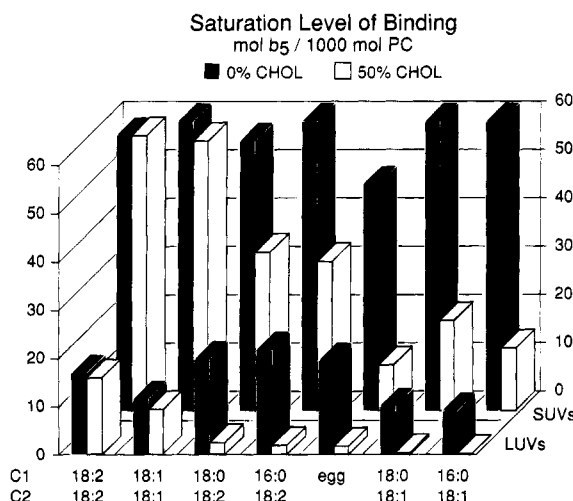


FIGURE 5: Effects of curvature and lipid composition on cytochrome *b*₅ saturation of liposomes.

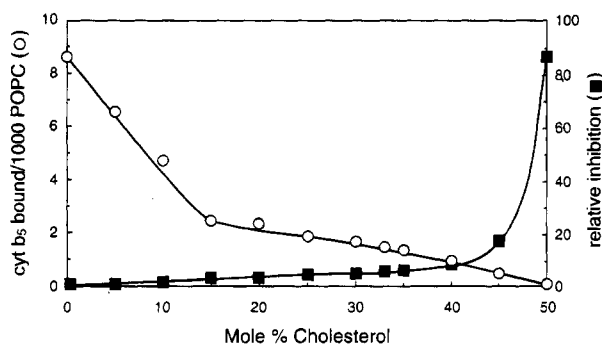


FIGURE 6: Cytochrome *b*₅ interaction with POPC LUVs as a function of cholesterol composition. Cytochrome *b*₅ (0.048–0.08 μ mol) was incubated with POPC LUVs [4–20 μ mol of POPC doped with (8.0×10^4) – (1.9×10^5) dpm of [³H]triolein/ μ mol POPC] under argon in Tris–acetate buffer, pH 8.1, for 24 h at 30 °C. The initial cyt *b*₅:POPC mole ratio was varied between 1:50 and 1:417. Proteoliposomes were separated from unbound protein on Sepharose 2B-CL columns (0.9×28.5 cm or 1.6×55 cm) thermostated at 25 °C. (○) Saturation levels of cyt *b*₅ binding versus liposome cholesterol content. The saturation levels have been corrected for the liposome lamellarity as determined from TNBS labeling experiments. The reported values have an uncertainty of $\pm 3.5\%$. (■) Inhibition of cyt *b*₅ binding to POPC LUVs as a function of cholesterol mole percent. The reduction in cyt *b*₅ binding is expressed in terms of the cholesterol inhibitory parameter, ϕ , where $\phi = (\text{cyt } b_5/1000 \text{ POPC without cholesterol})/(\text{cyt } b_5/1000 \text{ POPC with cholesterol})$.

(Greenhut *et al.*, 1993; Taylor, 1993). In the absence of cholesterol, approximately 15% of the bound protein becomes tightly inserted after a 2 h incubation with POPC LUVs at 30 °C. The rate of tight insertion increases with increasing cholesterol, reaching a maximum at 25 mole percent, and then decreases to the original rate in vesicles containing 50 mole percent cholesterol. These phenomena have been described in preliminary form (Taylor & Roseman, 1993; Taylor, 1993).

To determine if tight insertion enhances liposome saturation levels the extent of cyt *b*₅ binding to POPC LUVs with 25 mole percent cholesterol at various time intervals was examined. We have found that with these liposomes, the fraction of bound cyt *b*₅ that is tightly inserted is 50% after 2 h, and 100% after 24 h (Taylor & Roseman, 1993; Taylor, 1993). If tight binding enhances the saturation level, an increase in protein binding should be observed over the 2–24

Table 3: Effect of Cholesterol on Cytochrome *b*₅ Binding to POPC LUVs^a

cholesterol (mol %)	K_{eff}^b ($\times 10^4$) (M^{-1})	n^c	K_p^d (M^{-1})	s^e (cyt <i>b</i> ₅ / 1000 PL)	ϕ^f
0	9 ± 1	161 ± 6	600 ± 60	6.2 ± 0.2	1.0
10	9 ± 1	280 ± 10	320 ± 30	3.6 ± 0.1	1.7 ± 0.2
20	8 ± 1	590 ± 20	140 ± 14	1.7 ± 0.06	3.6 ± 0.6
40	9 ± 1	670 ± 30	130 ± 13	1.5 ± 0.07	4.1 ± 0.8

^a Determined by Scatchard analysis. The protocol was essentially the same as described under Experimental Procedures for cyt *b*₅ binding to SUVs except for the following modifications: (1) Excitation beam attenuation was adjusted by multiplying the obtained fluorescence spectra by the factor $\text{antilog } A_{280}/2$, where A_{280} is the 280 nm optical density of specific concentrations of LUVs and (2) the relative binding lattice sizes and the corresponding geometrical parameters λ , α , and γ were determined from the saturation studies (Figure 6) using eqs 4, 5, and 6. ^b Effective affinity constant for a binding "site" on a liposome. ^c Phospholipids per site. ^d Affinity constant for a phospholipid (K_{eff}/n). ^e Cyt *b*₅ saturation level of a liposome, n^{-1} , uncorrected for liposome lamellarity. ^f Cholesterol inhibitory parameter, (cyt *b*₅ saturation in liposomes without cholesterol)/(cyt *b*₅ saturation in liposomes with cholesterol).

h time interval when vesicles are incubated with an excess of protein. No increase was observed, indicating that each binding form requires the same number of phospholipids per site.

DISCUSSION

The present investigation demonstrates that bilayer curvature, fatty acyl composition, and cholesterol content significantly affect cyt *b*₅ partitioning into preformed liposomes. The following observations have been made:

(i) The saturation limits of SUVs are considerably greater (up to 7-fold) than those of LUVs. For most of the cholesterol-free SUVs, the average saturation level of binding is approximately 18 phospholipids per cyt *b*₅, corresponding to approximately 11 PL/*b*₅ in the outer monolayer. A binding site of this size is consistent with the assumptions for the binding lattice model on an SUV. A model of a protein-saturated SUV indicates that the cyt *b*₅ molecules are almost at the limit of packing density (Figure 7). In contrast, the distances among proteins on the LUV surfaces are surprisingly large.

(ii) The affinity constants are greater for SUVs that are prepared from phospholipid mixtures than for SUVs of a single phospholipid component.

(iii) Cholesterol decreases the cyt *b*₅ saturation level and the binding affinities of all liposomes. The binding inhibition is much greater with LUVs than with SUVs, and it is also highly sensitive to the distribution and number of double bonds in the fatty acyl chains of the phospholipids. On a per mole basis, the studies of cyt *b*₅ interaction with POPC LUVs indicate that the most significant binding inhibition occurs at cholesterol compositions that are greater than 33 mole percent.

Most of these results may be rationalized in a similar manner as suggested by Marqusee and Dill (1986) and DeYoung and Dill (1988) in their studies of small molecule partitioning into bilayers. Using a mean field lattice theory, they were able to account for their observation that the equilibrium partitioning of solutes into bilayers is reduced as the surface density of the lipid increases. Surface density can be increased by lowering the temperature, altering the acyl chain composition, and adding cholesterol. The theory

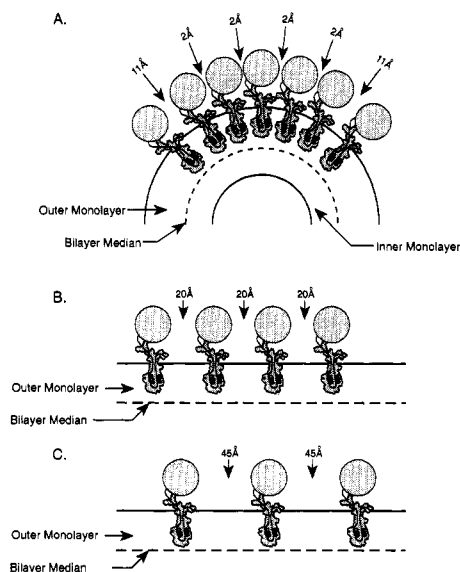


FIGURE 7: Model of cytochrome b_5 packing in liposomes at saturation. (A) SUVs; (B) LUVs (PLPC, egg PC); and (C) LUVs (POPC). The average distances between cyt b_5 molecules in the exterior monolayer were calculated from the limiting molecular areas of the individual phosphatidylcholines (Jain, 1988) and the assumption of 14.6 Å as the minimum radius for a perfectly spherical cyt b_5 catalytic domain (Visser *et al.*, 1975) according to the formula: distance = $(\sqrt{(PL/b_5)(\text{area}/PL)/\pi} - [b_5 \text{ radius}]) \times 2$ where PL/b_5 is the number of phospholipids per protein in the exterior monolayer of a liposome.

predicts that solute expulsion should result from the entropy loss that accompanies ordering of phospholipid chains around the solute.

The potential importance of lipid packing density (or related packing parameters) on the physical properties of proteins in bilayers was investigated by Litman and co-workers (Mitchell *et al.*, 1990) in studies of the effect of phospholipid composition, cholesterol, and temperature on the metarhodopsin I \rightleftharpoons metarhodopsin II equilibrium. They found that the meta I \rightarrow meta II conversion, which requires expansion of the protein, correlates with the bilayer free volume available for unhindered motion of fluorescent probes.

It seems reasonable to further suggest that any factor which reduces the conformational flexibility of the lipid, such as the substitution of cholesterol for phospholipid, would limit the ways in which lipid molecules could pack against the protein, and thereby decrease the solubility of the protein in the bilayer. In contrast, factors that increase lipid disorder, such as reduced liposome size (i.e., increased curvature) and increased compositional heterogeneity, should favor protein solubility. Most of our results can be qualitatively accounted for in this way.

The large changes in cytochrome b_5 binding cannot be correlated directly with the relatively small changes that can occur in lipid packing density or area per molecule. For example, addition of equimolar cholesterol to egg PC bilayers produces a maximum reduction of area/PC of approximately 20% (Lecuyer & Dervichian, 1969). Similarly, the area change per lipid molecule at the phase transition is $\approx 20\%$, corresponding to a volume change of only 5% (Cevc & Marsh, 1987). These small changes reflect the fact that fluid lipid bilayers are condensed phases, wherein the lipids cannot be packed much more tightly. Bilayers have a small free

Table 4: Condensation of Lipids in Monolayers of Equimolar Phospholipid and Cholesterol:^a Correlation with Reduction in Cytochrome b_5 Binding to LUVs

phospholipid		A_{ideal}	A_{obs}	$A_{\text{ideal}}/A_{\text{obs}}$	A_{min}^b	$A_{\text{f,ideal}}/A_{\text{f,obs}}^c$	ϕ
C1	C2	(Å ²)	(Å ²)		(Å ²)		
18:2	18:2	68.7	68.7	1.00	44.3	1.00	1.00
18:1	18:1	64.0	58.7	1.09	44.3	1.36	1.20
16:0	18:2	61.0	51.0	1.20	44.3	2.42	12.2
18:0	18:1	58.0	46.0	1.26	44.3	7.00	51.5

^a Data in columns 1–4 were taken directly from Figure 8A of Demel *et al.* (1972) and from Figure 8 of Demel *et al.* (1967). A_{obs} is the observed mean area per molecule of the equimolar phospholipid/cholesterol mixtures at 12 dyn/cm and 22 °C; A_{ideal} is the area per molecule that would be observed if the areas of the phospholipids and cholesterol were simply additive. In the fifth column, the magnitude of the condensing effect (deviation from ideal mixing) is expressed as the ratio of these two areas. ^b A_{min} is the mean minimum area per molecule, as determined from areas of cholesterol and phospholipid at the collapse pressure. As shown in Table 1 of Joos and Demel (1969), the areas of the phospholipids listed above are essentially the same (± 1 Å²) with an average of approximately 53 Å². The limiting area of cholesterol is taken to be 35.5 Å² (average the reported 35–36 Å²). A_{min} for the equimolar mixture of cholesterol and phospholipid was assumed to be the average of the individual limiting areas: $1/2(53 + 35.5) = 44.3$ Å². ^c The parameter A_{f} , the “free area,” is introduced. This is the area per molecule (ideal or observed) minus A_{min} . Since A_{f} is proportional to the free volume per phospholipid, A_{f} is a measure of the volume available for solute partitioning. See text for further explanation. The ratio $A_{\text{f,ideal}}/A_{\text{f,obs}}$ is therefore a measure of the factor by which the volume available for solute partitioning is reduced by the condensation effect. This is the most appropriate factor to correlate with ϕ (last column), the factor by which cytochrome b_5 binding is reduced.

volume. However, as cholesterol is added or as the bilayer is taken below the phase transition, the *relative* amount of free volume can be greatly reduced, as illustrated with the following numerical example. A phospholipid that occupies 1500 Å³ in the liquid-crystalline state and 1425 Å³ in the gel state has a free volume of $1500 - 1425 = 75$ Å³ above T_c . If some factor (such as cholesterol) reduces the molecular volume by 74 Å³, the packing density would increase by a factor of just $(1500/1425) = 1.05$, whereas the free volume would be reduced by a factor of 75 (from 75 to 1 Å³).

If the free volume is essentially the volume available for solute partitioning, there should be a correlation between this parameter and protein binding. Unfortunately, there is not sufficient bilayer data available to make such an analysis. However, the abundance of monolayer data makes it possible to correlate our results with changes in lipid areas. For this purpose, we have defined the following parameters, in analogy with those used to quantify changes in density: area per lipid molecule, A ; minimum area per lipid molecule, A_{min} ; and free area per lipid molecule, A_{f} . A_{min} is the area per lipid molecule at the collapse pressure, so that $A_{\text{f}} = A - A_{\text{min}}$, and is directly related to the molecular free volume.

To determine the importance of the condensing effect, it is necessary to compare experimentally observed values of the above parameters with theoretical results that are expected with an ideal (noncondensing) mixture of the lipids. In an ideal mixture, the areas of the individual components are simply additive; the average area per molecule is therefore a weighted average of the individual areas. Subscripts “ideal” and “obs” are used accordingly.

In Table 4 these areas are calculated for equimolar mixtures of cholesterol and synthetic phospholipids. $A_{\text{ideal}}/$

Table 5: Effect of Cholesterol in Reducing the Mean Molecular "Free Area" of Lipids in POPC Monolayers,^a and the Correlation with Inhibition of Cytochrome *b*₅ Binding to POPC LUVs

X_{chol}	$A_{\text{ideal}} (\text{\AA}^2)$	$A_{\text{obs}} (\text{\AA}^2)$	$A_{\text{min}}^b (\text{\AA}^2)$	$A_{\text{f,ideal}} (\text{\AA}^2)$	$A_{\text{f,obs}} (\text{\AA}^2)$	$A_{\text{f,0\%chol}}/A_{\text{f,ideal}}$	$A_{\text{f,0\%chol}}/A_{\text{f,obs}}$	ϕ
0	65.8	65.8	54.0	11.8	11.8	1.00	1.0	1.0
0.1	63.1	60.3	52.1	11.0	8.2	1.07	1.4	1.8
0.2	60.4	54.9	50.3	10.1	4.6	1.16	2.6	3.6
0.3	57.6	51.5	48.4	9.2	3.1	1.28	3.8	5.1
0.4	54.9	48.1	46.6	8.3	1.5	1.42	7.9	8.7
0.5	52.2	45.0	44.7	7.5	0.3	1.57	40	87

^a Mean molecular areas shown in columns 2 and 3 were calculated from Table 2 of Ghosh and Tinoco (1972), where deviations from ideal mixing ($A_{\text{ideal}} - A_{\text{obs}}$) are reported for $X_{\text{chol}} = 0, 0.2, 0.4, 0.6, 0.8$, and 1.0 at 40 dyn/cm and 22°C . The observed molecular areas of cholesterol and POPC at this pressure are 38.6 and 65.8 \AA^2 , respectively. Consequently, $A_{\text{ideal}} = X_{\text{chol}}(38.6) + X_{\text{POPC}}(65.8)$. Data shown here for $X_{\text{chol}} = 0.1, 0.3$, and 0.5 were calculated by interpolation. $A_{\text{f,ideal}} = A_{\text{ideal}} - A_{\text{min}}$; $A_{\text{f,obs}} = A_{\text{obs}} - A_{\text{min}}$. ^b Minimum molecular areas were taken from Table 1 of Joos and Demel (1969). For the lipid mixtures, $A_{\text{min}} = (X_{\text{chol}})(A_{\text{min, chol}}) + (X_{\text{POPC}})(A_{\text{min, POPC}})$. From the reported range of $35\text{--}36 \text{ \AA}^2$ for cholesterol, we used the average $= 35.5 \text{ \AA}^2$ in our calculations. Although no measurements with POPC were performed, $A_{\text{min}} = 54 \text{ \AA}^2$ was reported for the close structural analog oleoylstearyl-PC. We assume that the same value is applicable to POPC, since A_{min} does not vary significantly with structure for lecithins having one or more double bonds (A_{min} for both dioleoyl- and dilinoleoyl-PC is 53 \AA^2). To construct Table 5, a value of A_{min} to three significant figures was chosen, $= 54.0 \text{ \AA}^2$; otherwise, rounding A_{min} at $X_{\text{chol}} = 0.5$ to two significant figures ($= 45 \text{ \AA}^2$) would make $A_{\text{f,obs}} = 0$, and therefore $A_{\text{f,POPC}}/A_{\text{f,obs}}$ would $= \infty$. Clearly, the uncertainty in $A_{\text{f,obs}}$ and therefore in the ratio $A_{\text{f,POPC}}/A_{\text{f,obs}}$ becomes very large as, in this case, A_{obs} approaches A_{min} . The smallest estimate of $A_{\text{f,POPC}}/A_{\text{f,obs}}$ is obtained by using A_{min} 's at the low end of the range for cholesterol and POPC. If these are assumed to be 35 and 53 \AA^2 , respectively, $A_{\text{f,POPC}}/A_{\text{f,obs}} = 12$. Choosing values of A_{min} only slightly greater than those employed (such as 54.5 \AA^2 instead of 54 \AA^2 for POPC) results in $A_{\text{f,obs}} = 0$, and $A_{\text{f,POPC}}/A_{\text{f,obs}} = \infty$.

Table 6: Effect of Cholesterol in Reducing the Mean Molecular "Free Area" of Lipids in Egg PC Bilayers^a

X_{chol}	$A_{\text{ideal}} (\text{\AA}^2)$	$A_{\text{obs}} (\text{\AA}^2)$	$A_{\text{min}}^b (\text{\AA}^2)$	$A_{\text{f,ideal}} (\text{\AA}^2)$	$A_{\text{f,obs}} (\text{\AA}^2)$	$A_{\text{f,0\%chol}}/A_{\text{f,ideal}}$	$A_{\text{f,0\%chol}}/A_{\text{f,obs}}$
0	61.4	61.4	48.0	13.4	13.4	1.00	1.0
0.1	59.0	56.2	46.9	12.1	9.3	1.11	1.4
0.2	56.5	51.5	45.8	10.7	5.7	1.25	2.4
0.3	54.1	46.7	44.7	9.4	2.0	1.43	6.7
0.4	51.6	44.3	43.6	8.0	0.7	1.68	19
0.5	49.2	42.7	42.5	6.7	0.2	2.00	67

^a Mean molecular areas, A_{obs} , were calculated from the molecular areas of egg PC, A_{eggPC} , shown in Figure 6 of Lecuyer and Dervichian (1969), and from the authors' conclusion that cholesterol adds 37 \AA^2 at all mole fractions. Consequently, $A_{\text{obs}} = X_{\text{eggPC}}A_{\text{eggPC}} + X_{\text{chol}}(37)$; $A_{\text{ideal}} = X_{\text{chol}}(37) + X_{\text{eggPC}}(61.4)$. ^b The authors argue that the limiting area for egg PC is 48 \AA^2 . With this assumption, the mean minimum molecular areas for the mixtures are $A_{\text{min}} = X_{\text{chol}}(37) + X_{\text{eggPC}}(48)$.

A_{obs} is the customary measure of the magnitude of the condensing effect, and is directly proportional to the change in packing density. As shown in column 5, the maximal change in this ratio is 1.26. However, this modest increase is accompanied by a substantial, 7-fold reduction in free area (column 7). The reduction in free area correlates much better with the inhibition of protein binding (column 8) than does the increase in packing density. Though the discrepancies are still large, the changes are of comparable magnitude. In similar fashion, as shown in Table 5, the results from Figure 6 can be correlated with the loss of free volume as cholesterol is added to POPC LUVs.

The analysis described above is not intended to be rigorous, but simply to find a property of monolayers or bilayers that plausibly, and semiquantitatively, accounts for the observed trends in cyt *b*₅ binding inhibition. Discrepancies between predicted and observed values are not surprising, in view of the simplified model, and the use of monolayer data obtained at surface pressures much different from bilayers. Despite these reservations, the effect of cholesterol in reducing the free area of egg PC bilayers closely parallels the effect of cholesterol on POPC monolayers, as shown in Table 6. These results strongly suggest that the use of monolayer data is a reasonable approximation.

Although the effects of decreasing vesicle curvature or increasing cholesterol content on the binding *affinities* of a solute could be readily explained by acyl chain conformational restrictions, it is more difficult to account for the large reduction in the *saturation levels* of cyt *b*₅ binding. For a

pure POPC LUV, the calculated lipids per site in the outer monolayer is 55, and for a POPC LUV with 50% cholesterol, the phospholipids per binding site is 4950. The result in the absence of cholesterol coincides with NMR studies showing that cyt *b*₅ perturbs approximately 50 phospholipids in DPPC bilayers (Füldner, 1980). To explain the NMR results, Sackmann *et al.* (1984) suggested that cyt *b*₅ locally deforms the bilayer, creating a dimple that involves several lipid layers. Perhaps interactions between cholesterol and certain phospholipids sufficiently stabilize the bilayer from such putative perturbations or deformations by the protein. [For a more recent discussion of long-range effects of protein on surrounding lipid, see Lentz (1988)].

The results of this study may help to explain the apparently disparate observations reported in the literature concerning cholesterol-protein interactions. If our results are generally applicable, the effect of cholesterol on the chemical potential of a membrane protein is highly dependent upon the cholesterol content and other variables such as the chemical composition of the phospholipid and the size (i.e., curvature) of the liposomes. Consequently, the variety of results reported may simply reflect differences among experimental conditions.

Our results suggest that lipid composition can substantially affect the chemical potentials of integral proteins in biological membranes. It is remarkable to find that the inner monolayer of plasma membranes can contain as much as 65 mole percent cholesterol (Wood *et al.*, 1990; Sweet & Schroeder, 1988). At this level of cholesterol, the aggregation state of

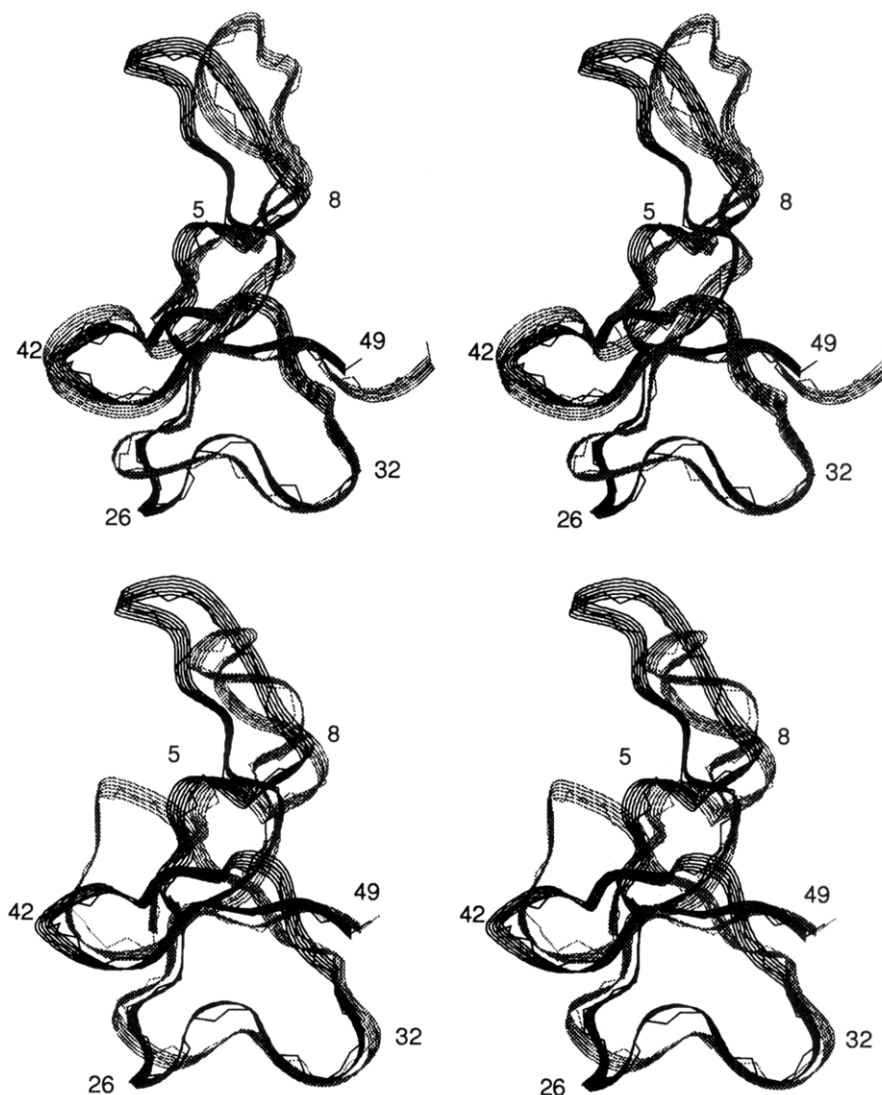


FIGURE 9: Stereoviews of superpositions of the structures of AP-A and Sh I (upper) and AP-A and ATX Ia (lower). In each case AP-A is the darker shaded structure. For AP-A the structure which is closest to the average is shown (cf. Figure 8), while for Sh I the closest to the average of the minimized 'new' structures of Wilcox et al. (1993) is shown and for ATX Ia the lowest energy structure of Widmer et al. (1989). The structures were superimposed over the backbone heavy atoms of residues 2–6, 20–24, 27–36, and 45–49 in AP-A, corresponding to 2–6, 20–34, and 42–46 in ATX Ia and 1–5, 19–33, and 42–46 in Sh I. Residue numbers on the structures are those of AP-A.

sheet making the major contribution to the hydrophobic core of the molecule (Figure 3). The solvent accessibilities of the indole rings of the three Trp residues, which form part of this core, can be compared with previous observations using photochemically-induced dynamic nuclear polarization (Norton et al., 1986), which showed that Trp33 and Trp45 were accessible to the water-soluble flavin dye used in these experiments, whereas Trp23 had limited access. In our structures the accessibilities of the entire indole rings were in the order $\text{Trp45} > \text{Trp23} \geq \text{Trp33}$, whereas the accessibilities of the indole NH groups were $\text{Trp33} > \text{Trp45} > \text{Trp23}$, with the Trp23 NH being completely inaccessible in all of the structures. This suggests that the accessibility of the indole NH may be of greater importance in the development of polarization in these experiments than the accessibility of the ring as a whole.

The aromatic rings of Trp23 and Trp33 are oriented such that the indole NH of Trp23 lies directly above the six-membered ring of Trp33. This no doubt accounts for the remarkable upfield shift of the Trp23 NH, from its expected position of 10.2 (Wüthrich, 1986) to 5.92 ppm. Burley and Petsko (1986) have shown that amino groups of Lys, Arg,

Asn, and Gln and imidazole NH groups of His are often found above and below aromatic rings and close to their center, where they make energetically favorable interactions with the π -electrons. The interaction of the indole NH of Trp23 with the π -orbital of the six-membered ring of Trp33 probably reflects a specific interaction of this type, supplemented by edge-to-face interactions of the two indole rings (Burley & Petsko, 1986). The mean distance of the Trp23 nitrogen from the centre of the six-membered ring of Trp33 is 3.1 Å, close to the optimal distance from an amino nitrogen to a ring centre (Levitt & Perutz, 1988), and the NH group points directly toward the ring.

Comparison with Other Long Sea Anemone Polypeptides. The overall fold of AP-A is very similar to those of the type 1 toxin ATX Ia (Widmer et al., 1989) and the type 2 toxin Sh I (Fogh et al., 1990; Wilcox et al., 1993), as shown in Figure 9. Mean pairwise rms differences between the 20 final structures of AP-A and the eight published structures of ATX Ia and the 12 minimized 'new' structures of Sh I are 1.48 and 1.54 Å, respectively, when superimposed over the backbone heavy atoms of residues 2–6, 20–24, 27–36, and 45–49 in AP-A, which correspond to 2–6, 20–34,